# SOLDER JOINT RELIABILITY OF FLIP CHIP BGA PACKAGE

BY

## LEE KOR OON

Thesis submitted in fulfillment of the

requirements for the degree of

Master of Science

**March 2004**

# ACKNOWLEDGEMENT

I would like to express my deepest gratitude to Professor K. N. Seetharamu, my main supervisor for his excellent guidance, support and counsel during the undertaking of this work.

I would also like to express my sincere thanks to my co-supervisor, Dr. Ishak Hj. Abdul Azid for his constant guidance, encouragement and support in helping me to finish the project.

Special thanks go to my fellow friend, Ong Kang Eu for guiding me with ANSYS$^{TM}$ in the initial stages of the work. Without his effort, this project would not have been completed.

Last by not least, I dedicate this work to my parents, for bringing me to where I am today.

THANK YOU!

**TABLE OF CONTENTS**

# LIST OF FIGURES

# LIST OF TABLES

# NOMENCLATURE

| | |
|---|---|
| T | Temperature |
| CTE | Coefficient of thermal expansion |
| $N_o$ | Thermal cycles to crack initiation |
| $\Delta W_{ave}$ | Change in plastic work |
| $\dfrac{da}{dN}$ | Crack propagation rate per thermal cycle |
| $\alpha_w$ | The characteristic solder joint fatigue life |
| $a$ | Solder joint diameter |
| $\dfrac{d\varepsilon_p}{dt}$ | Effective inelastic deformation rate |
| $s$ | Initial value of deformation resistance |
| $Q/k$ | Activation energy/Boltzmann's constant |
| $A$ | Pre-exponential factor |
| $\xi$ | Multiplier of stress |
| $m$ | Strain rate sensitivity of stress |
| $h_o$ | Hardening constant |
| $s^\wedge$ | Coefficient for deformation resistance saturation value |
| $n$ | Strain rate sensitivity of saturation value |
| $a'$ | Strain rate sensitivity of hardening |
| $\dfrac{d\varepsilon_s}{dt}$ | Steady state strain rate |
| $k$ | Boltzmann's constant |
| $\sigma$ | Applied stress |
| $Q_a$ | Apparent activation energy |

| | |
|---|---|
| $n$ | Stress exponent |
| $\alpha$ | Stress level at which the power law dependence breaks down |
| $\varepsilon_c$ | Creep strain |
| $\varepsilon_T$ | Transient creep strain |
| $B$ | Transient creep coefficient |
| $\varepsilon_p$ | Time-independent plastic strain |
| $G$ | Shear modulus |
| $C_{ss}$, $C_p$, $m_p$ | Constants |
| $\varepsilon_{in}$ | Total inelastic strain |

## Subscripts

| | |
|---|---|
| ave | average |

**ABSTRAK**

Daya tahan hubungan bebola pateri merupakan satu kriteria keboleharapan yang penting dalam pempakejan elektronik moden. Untuk mengurangkan kos pembangunan dan memaksimumkan performasi ketahanan pakej elektronik, analisis termaju menjadi satu keperluan dalam fasa rekabentuk dan pembangunan pakej mikroelektronik. Simulasi analitikal komputer seperti analisa unsur terhingga boleh memberi satu gambaran terperinci tentang taburan dan sejarah tegangan/tegasan pateri di bawah pelbagai bebanan yang berbeza. Ia juga merupakan satu alat pengoptimuman yang sesuai untuk melakukan kajian parametrik.

Analisa unsur terhingga tiga dimensi digunakan untuk menentukan respon kelesuan hubungan pateri suatu pakej di bawah keadaan perubahan suhu berulang-alik terpecut. Oleh kerana terdapat perbezaan dalam kadar pengembangan haba bagi setiap bahan yang digunakan untuk menghasilkan suatu pakej, perubahan suhu menyebabkan ketidakseimbangan pengembangan pakej dan seterusnya menyebabkan tegasan hubungan bebola pateri. Penghasilan tegasan tersebut yang berulang kali akhirnya menyebabkan kegagalan hubungan pateri, suatu mekanisma yang biasanya dikenali sebagai kelesuan berulang-alik rendah.

Struktur bebola pateri menampung kebanyakan daripada ketegangan plastik yang dihasilkan semasa perubahan suhu berulang-alik terpecut. Oleh sebab ketegangan plastik merupakan parameter dominan yang mempengaruhi kelesuan berulang-alik rendah, ia digunakan sebagai asas evaluasi untuk menentukan keboleharapan struktur bebola pateri. Satu kaedah peramalan jangka hayat bebola pateri yang telah diterbitkan akan digunakan di mana hasil keputusan daripada simulasi kaedah unsur terhingga diterjemah kepada ramalan jangka hayat untuk kegagalan. Kajian ini membincangkan

kaedah analisis seperti yang dilaksanakan dalam perisian komputer kaedah simulasi unsur terhingga ANSYS$^{TM}$ dan juga keputusan jangka hayat bebola pateri pakej yang dihasilkan. Rangkaian Neural Tiruan (ANN) akan digunakan untuk melengkapkan kajian parameter dan seterusnya Algoritma Genetik (GA) akan digunakan untuk menyiasat gabungan parameter-parameter yang diperlukan bagi suatu jangka hayat yang tertentu.

## ABSTRACT

The integrity of ball and bump solder joints is a major reliability concern in modern micro electronic packages. To minimize development costs and maximize reliability performance, advanced analysis is a necessity during the design and development phase of a microelectronic package. Computer simulation such as finite element analysis can provide a very detailed description of solder stress/strain distribution and history under a variety of loading conditions, and it is a powerful tool for performing parametric studies and design optimization.

Three-dimensional finite element analysis has been applied to determine the time-dependent solder joint fatigue response of a package under accelerated temperature cycling conditions. Due to the difference in the thermal expansion of the various materials involved in the construction of a typical package, temperature variations create a mismatch in package expansion which ultimately results in solder joint stress. Repeated application of this stress eventually causes solder joint failure, a mechanism commonly known as low cycle fatigue.

The solder structures accommodate the bulk of the plastic strain that is generated during accelerated temperature cycle. Since plastic strain is a dominant parameter that influences low-cycle fatigue, it is used as a basis for evaluation of solder joint structural integrity. An extensively published and correlated solder joint fatigue life prediction methodology was incorporated by which finite element simulation results were translated into estimated cycles to failure. This study discusses the analysis methodologies as implemented in the ANSYS$^{TM}$ finite element simulation software tool and the corresponding results for the solder joint fatigue life. Artificial Neural Network (ANN) has been used to consolidate the parametric studies and then the evaluation of

parameters to give a particular fatigue life is achieved by the use of Genetic Algorithm (GA).

**CHAPTER 1**

**INTRODUCTION**

## 1.1 Flip Chip Technologies

Flip chip technology, in the book edited by Lau (Lau, 1995) is defined as placing a chip to the substrate by flipping over the chip so that the I/O area of the chip is facing the substrate. By flipping over the chip, the interconnection between the chip and the substrate are achieved by conductive "bumps" placed directly in between the die surface and the substrate. Therefore, the whole chip surface can be utilized for active interconnections and at the same time, eliminates the need for wire bonding.

An internet source, (FlipChips Dot Com, 2001) indicates that flip chip interconnection has been introduced since the early sixties by IBM for use in their mainframe computers and IBM has continued to use flip chip up to the present day. The same source also acknowledges the role played by Delco Electronics in helping to develop flip chip for automotive applications in the seventies. These early developments together with the advantages of flip chip packaging technology which offers smaller chip size, higher I/O density with area array, better electrical performance and lowest cost interconnection for high volume automated production results in flip chip packaging being considered as the preferred choice over other conventional wafer level packaging technology (Meilhon et al., 2003).

## 1.2 Solder Joint Reliability

There are essentially three basic elements in the solder flip chip interconnect systems (Fig. 1.1). These include the chip, the solder bump, and the substrate. The solder bumps in a flip chip interconnect system has three functions. First, the solder

joint forms the electrical connection between the chip and the substrate. Second the solder joint also serve as a path for heat dissipation from the chip.
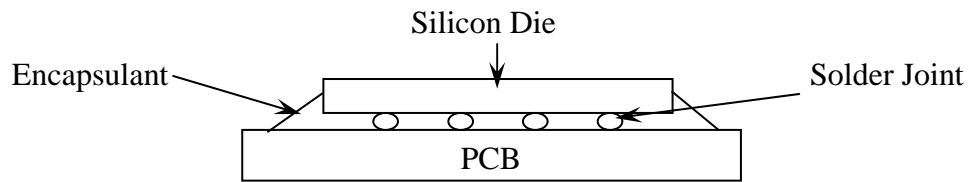


**Fig. 1.1** Schematic of a solder flip chip interconnect system (Pang, 2001a)

Lastly, the solder joint provides the structural link between the chip and the substrate. The structural integrity of the solder joint affects both the electrical and thermal performances of the flip chip interconnect system. Degradation in the structural integrity can be a reliability concern.

Another reliability concern is the thermo-mechanical behaviour of the solder joint. Thermal mismatch deformations due to the different coefficient of thermal expansion (CTE) between different materials used in the package can cause mechanical stresses in the solder joint. This will eventually cause crack growth and leads to failure in the package.

## 1.3 Finite Element Simulation

The effect of temperature cycling on the reliability of microelectronic packages has been the subject of many studies. Because of the difference in the thermal expansion of the multiple materials involved in the construction of a typical package, temperature variations create a mismatch ultimately resulting in solder joint stress. Repeated application of this stress eventually causes solder joint failure, a mechanism commonly known as low cycle fatigue.

To minimize development costs and maximize reliability performance, advanced analysis is a necessity during the design and development phase of a microelectronic package. Computer simulation such as finite element analysis can provide a very detailed description of solder stress/strain distribution and history under a variety of loading conditions, and is a powerful tool for performing parametric studies and design optimization. However, analyst is typically interested in the cycles to failure that a package design configuration and cyclic loading condition will cause. This requires the utilization of a life prediction methodology in which data typically provided by a finite element solution can be translated into cycles to solder joint failure.

## 1.4 Artificial Neural Network (ANN)

Artificial Neural Network is a system loosely modeled based on the human brain. Among the names frequently encountered in the field are connectionism, parallel distributed processing, neuro-computing, natural intelligent systems, machine learning algorithms, and artificial neural networks (Klerfors, 1998).

An artificial neural network operates by establishing links between many different processing elements, each akin to a single neuron in the natural brain. Each neuron receives many input signals, then, based on an internal weighting system produces a single output signal that's usually sent as input to another neuron. The neurons are closely interconnected and organized into different layers. The input layer receives the input, the output layer produces the final output. Usually one or more concealed layers are sandwiched in between the two. This configuration makes it impossible to predict or know the exact flow of data.

ANNs normally begin with randomized weights for all their neurons. This means that they don't "know" anything and must be taught to solve the particular

problem for which they are intended. Generally speaking, there are many learning laws by which ANN can learn, such as Hebb's Rule, Hopfield Law, The Delta Rule, and Kohenen's Learning Law (Klerfors, 1998), depending on the problem it must solve. A self-organizing ANN (often called a Kohonen after its inventor) is exposed to large amounts of data and tends to discover patterns and relationships in that data. Researchers often use this type to analyze experimental data. A back-propagation ANN, conversely, is trained by humans to perform specific tasks. During the training period, the user evaluates whether if the ANN's output is accurate. If it's accurate, the neural weightings that produced that output are reinforced; if the output is incorrect, those weightings responsible are diminished. This type is most often used for cognitive research and for problem-solving applications.

## 1.5 Genetic Algorithm (GA)

Genetic Algorithm (GA) as described in the book by Goldberg (Goldberg, 1997) is an adaptive search method based on Darwin's principles of natural selection, survival of the fittest and natural genetics. They combine survival of the fittest among string structures with a well-organized random information exchange to form a search algorithm very comparable to some of the innovative flair of human search. As in human genetics, GA exploits the fittest traits of old individuals to create a new generation of artificial creatures (strings). With each generation, a better population of individuals is created to replace the old population. Based on these principles, genetic algorithm is developed as a search tool that efficiently exploits historical information to speculate on new search points with expected improved performance.

The genetic algorithm determines which individual should survive, which should reproduce and which should die. It also records statistics and decides how long the

evolution should continue. In GA, a population of individuals (parents) within a machine represented by chromosomes is generated. Each individual in the population represents a possible solution to a given problem. The individuals in the population then go through a process of evolution. This process of evolution involves each individual being evaluated and given a fitness score according to how well it is suited to be a solution to the problem. Individuals with a high fitness score will be selected and allowed to reproduce with other individuals in the population. The properties of each individual are described by using a chromosome and reproduction within individuals occurs through the crossover and mutation process. These two processes produce new individuals that will become the new population of solutions for the next generation. Members of the population with a low fitness score will be discarded and are unlikely to be selected for the next evolution process.

The entire process of evaluation and reproduction then continues until either the population converges to an optimal solution for the problem or the genetic algorithm has run for a specific number of generations.

With these capabilities, GA will be applied together with ANN as a tool for search and optimization purposes.

## 1.6 Literature Survey

Advances in the electronic industry leave in its wake a trail of reliability problems. The integrity of ball and bump solder joints is one of the major reliability concerns in modern microelectronic packages. A wide variety of literature is scanned for work done in addressing the reliability issues in microelectronic packages, particularly on the solder joint interconnect system. The search results indicate that quite a substantial amount of work has been done in this area since the last two decades.

In more recent years, many studies have been done on thermal stress/strain analysis on microelectronic packages. Li et al. (2003) utilized digital image correlation technique to obtain the deformation field of a Ball Grid Array (BGA) package. The results enable the authors to determine the strain/shear stress distribution of the package under thermal loading. More direct study on the solder joint itself has also been carried out by means of experimental work and computer simulations. Finite element analysis has in the past few years become a popular and powerful tool for researchers tackling the reliability issue of microelectronic packages.

Beh et al. (2003) utilized commercial finite element analysis software, ABAQUS to study the second level solder joint reliability risk of a Flip Chip Ball Grid Array (FCBGA) in temperature cycling reliability test. The effects of different ball grid array pattern and board thickness on the solder joint reliability of the FCBGA package have also been investigated.

Tee et al. (2003a) studied the design optimization of wafer-level Chip Scale Package (CSP) for improved solder joint reliability performance with fatigue modeling. Here the authors utilized a fatigue model based on a modified Darveaux's approach with non-linear viscoplastic analysis of solder joints (Darveaux, 1997; Darveaux, 2000). Design analysis is also performed on several critical design parameters.

Tee et al. (2003b) established a creep model for Thin-profile Fine-pitch Ball Grid Array (TFBGA) on board by PAKSI, a customized solder joint fatigue modeling software, to predict the fatigue life of solder joint during thermal cycling test. A parametric study on the design analysis of TFBGA was also carried out.

Stoyanov et al. (2001) applied computational modeling for flip chip assemblies where thermo-mechanical simulations were used together with numerical optimization and approximation techniques. The authors detailed the modeling integration approach

taken between the computational mechanics code-*PHYSICA*, and design optimization tool-*VisualDOC*.

Pang et al. (2001a) adopted a phenomenological approach in thermal analysis in which time independent plasticity and time dependent creep deformations are modeled separately. The phenomenological approach adopted by Pang describes the selectiveness of implementation (hence phenomenological) of the time independent plasticity and time dependent creep analysis in the author's two methods of analysis namely the dwell creep and full creep methods. Plasticity is defined by the propensity of a material to undergo permanent deformation under load. Time dependent plasticity and time independent plasticity indicates plasticity behaviour that either depends on time or independent of time. The full creep analysis models creep deformations during the temperature ramps as compared to the dwell creep analysis which omits creep behaviour during temperature ramps. A comparison was made with a rate dependent viscoplastic analysis approach. When creep is taken into consideration together with plasticity, then the term viscoplastic is defined. Therefore a rate dependent viscoplastic analysis indicates the analysis of time-dependent creep behaviour and time-dependent plastic behaviour.

Pang et al. (2001b) investigates the effects of employing different two-dimensional (2-D) and three-dimensional (3-D) finite element analysis (FEA) models for analyzing the solder joint reliability performance of a flip chip on board assembly. The FEA models investigated were the 2-D-plane strain, 2-D-plane stress, 3-D-1/8th symmetry and 3-D-strip models. Results indicate that the 2-D-plane strain and 2-D-plane stress model simulation have the highest and lowest strain in solder respectively. The 3-D-1/8th symmetry model gave solder strain results closer to the 2-D-plane strain

model, while the 3-D-strip model results fall closer to the 2-D-plane stress model. The 3-D results are clearly bounded by the 2-D-plane strain and 2-D-plane stress results.

Chandran et al. (2000) studied the reliability of solder joints by observing BGA fatigue failures on different test vehicles. Finite element analysis and physical failure analysis were used to determine the risk to the product. A parametric finite element analysis was also carried out to determine the effect of design features and package BGA layout pattern on the propensity of fatigue failure.

Zahn (2000a) applied three-dimensional finite element analysis to determine the time-dependent solder joint fatigue response of a tape based chip scale package under accelerated temperature cycling conditions. The effects of differing ball via configurations due to variations in both package assembly and tape vendors were also investigated.

Zahn (2000b) utilized viscoplastic finite element simulatioin methodologies to predict ball and bump solder joint reliability for a silicon based five-chip multi-chip module package under accelerated temperature cycling conditions. The analysis utilized the ANSYS sub-modeling methodology by which global model simulation results were applied as boundary conditions in localized sub-models of the solder balls and bumps.

Zahn (2000c) studied the effect of multiple die attach material configurations on the solder joint reliability for a same die size, stacked, chip scale, ball grid array package under accelerated temperature cycling conditions by using viscoplastic finite-element simulation methodologies.

Yao et al. (1999) developed two dimensional and three dimensional finite element models to numerically predict the stress, total strain, plastic strain, and cumulative plastic strain of the solder joints in an ATC 4.1 flip chip test vehicle, a microBGA, and a Chip Scale Package under temperature cycling. These stress and

strain values have been used to predict the solder joint lifetime through either strain-based approaches such as Coffin-Manson and modified Coffin-Manson equations, or stress-based approach (*S-N curve*).

Many more studies have been done on the issue of solder joint reliability and new findings are being constantly put forward for publications. It is clear that there are many challenges yet to be solved on the solder joint reliability. As solder joint interconnect remains the preferred choice for functionality and performance in today's microelectronic packages, many more work can be done to improve the reliability of solder joints. In view of this, a study of the solder joint reliability of a typical flip chip package will be carried out. It can be observed from the literature as well that some of the work involves parametric study as well. However, there has been no researcher so far that utilizes ANN and GA to consolidate his/her parametric analysis.

### 1.7 Objectives and Scope of Work

Many investigators have studied the low-cycle fatigue life of solder bumps under accelerated thermal cycling test (e.g. Popelar et al. (2000), Darveaux (2000), Zahn (2000a), Zahn (2000b), Wiese et al. (2001), Lau et al. (2002), Schubert et al. (2002), Dutta et al. (2002), & Schubert et al. (2003). It is true that many package configurations studied by these researchers roughly have the same build-up and each of the case studies utilizes a fatigue life prediction methodology not much different from one another. Even solder fatigue lives predicted fall within a certain common range of a few hundred cycles to a few thousand cycles. However, despite all these work, not a single analysis approach and results obtained for a case study can be directly used for another case study. There will be too many irregularities that must be accounted for in order to compare any two case studies. Hence, even if fatigue life prediction methodology using

plastic work is not new, different case study with different package configuration and different thermal cycle profile warrants the need for a simulation to be carried out in order to determine its solder fatigue life.

The objective of this work will be to predict the low-cycle fatigue life of a flip chip package subjected to two different accelerated temperature cycling test conditions. Temperature fluctuations caused by either power transients or environmental changes, along with the resulting thermal expansion mismatch between the various package materials, results in time and temperature dependent creep deformation of solder. This deformation accumulates with repeated cycling and ultimately causes solder joint cracking and interconnect failure. Due to the thermal mismatch in thermal expansion, plastic strain is generated during temperature cycling and the solder structures accommodate most of the plastic strain. Since plastic strain is a dominant parameter that influences low-cycle fatigue, it will be used as a basis for evaluation of solder joint structural integrity. An extensively published and correlated solder joint fatigue life prediction methodology based on viscoplastic finite element simulation will be incorporated by which finite element simulation results will be translated into estimated cycles to failure. Due to availability, the program ANSYS$^{TM}$ will be used to run the finite element simulations.

From the literature scan, many authors are also including package parametric analysis or package design optimization as part of their solder joint reliability investigations. However, most of the work on package parameter design analysis only involves further simulation with different package configurations. Therefore, in addition to the extra simulations, it is proposed that the Artificial Neural Network (ANN) be used as a tool to predict other data points in the simulation results. This will reduce the number of simulations required for parametric analysis.

ANN is a versatile prediction tool that can utilize existing simulation data for training and in the process be able to establish a connection between the input used in the training (package dimensions) and the output (solder joint fatigue life). By establishing this connection, ANN can be used to predict the output for other inputs other than those used in the training. ANN is also chosen because ANN does not depend on any governing equations and is able to give predictions based on raw data alone. Due to these reasons, ANN is a very suitable prediction tool to be utilized.

Parametric study in Chapter 4 is planned to be carried out by increasing or decreasing chosen package dimensions to study their effects on the solder joint fatigue life. In such scenario, the solder joint fatigue life can only be known after a simulation is carried out or after a prediction is made. Once the effects of every package dimensions on the solder fatigue life have been established, the solder fatigue life can be appropriately adjusted to a higher fatigue life or a lower fatigue life by increasing or decreasing a chosen package dimension. However, if the need arises that a certain solder fatigue life value is to be the target, how would one know what combination of package dimensions that can provide such a particular solder fatigue life? It is for this purpose that Genetic Algorithm (GA) is proposed to be used. Without any governing equations, and lacking the ability to work backwards from using the output (solder fatigue life) to predict the input (package dimensions), many optimization techniques cannot be utilized in such scenario. GA however can be linked up with ANN in order to make use of ANN's trained connection between the input and the output. By linking with ANN, GA can randomly provide a determined range of inputs for ANN to predict the output. If the output predicted is within the target output required, GA can easily store that set of inputs and their corresponding output and move on to another looped search.

**CHAPTER 2**

**METHODOLOGY**

**2.1 Solder-bumped Flip Chip Package**

A typical flip chip package measuring 14×14mm, with 256 solder balls (16×16 full ball matrix), 0.80mm pitch and attached to a 50×50mm board is analyzed. There are 2 dies in the package. The top die measured 9×9mm and the bottom die measured 12×12mm. The package outline drawing is shown in Fig. 2.1.
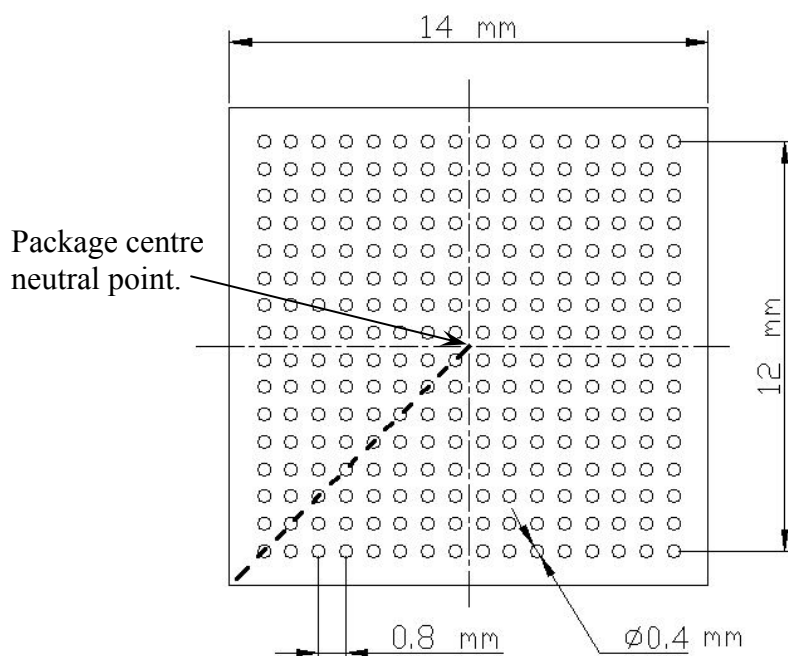


**Fig. 2.1.** Package outline drawing (Intel).

The basic structure of the solder-bumped flip chip package is shown in Fig. 2.2. More detailed layer dimensions of the package substrate and printed circuit board are shown in Figs. 2.3 and 2.4. Graphical details of the solder ball along with the package substrate pad and the printed circuit board pad are shown in Fig. 2.5. The stack-up layer dimensional information of the flip chip package is given in Table 2.1.
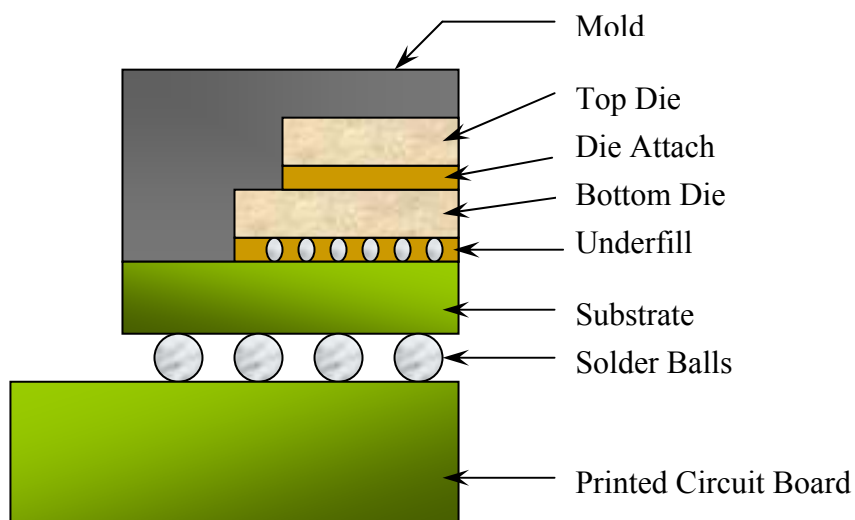
**Fig. 2.2.** Basic structure of a flip chip package (Intel).
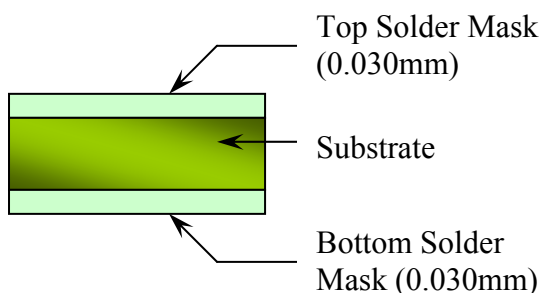


**Fig. 2.3.** Layer dimensions of package Substrate (Intel).
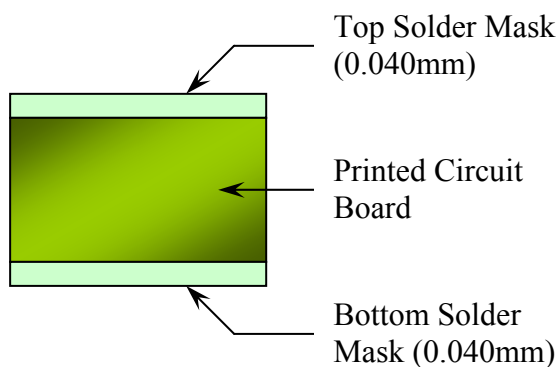
**Fig. 2.4.** Layer dimensions of printed circuit board (Intel).

As shown in Fig. 2.2, the basic structural layer layout of the typical flip chip package consists of the top die which is attached to the bottom die through the die attach layer. The bottom die is attached to the substrate through the underfill layer. Solder balls form the interconnection between the package substrate and the printed circuit board. The mold encompasses the top and bottom dies.
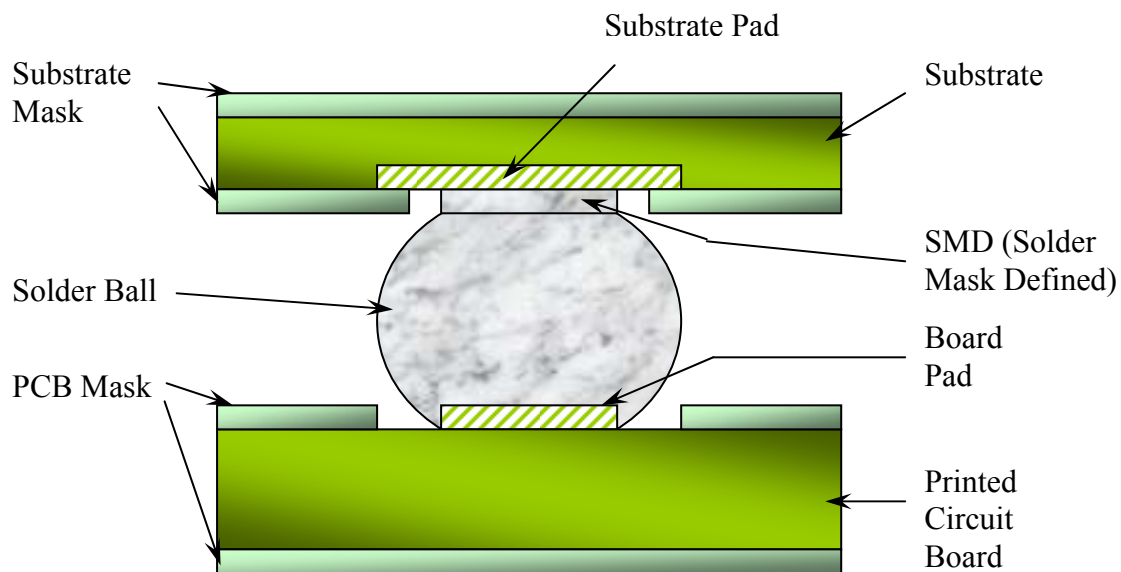
**Fig. 2.5.** Graphical details of the solder ball (Intel).

**Table 2.1.** Stack-up layer dimensions of the package (Intel).

| Package Attribute | | Dimension (mm) |
|---|---|---|
| Top Die | Thickness | 0.100 |
| | Size | 9×9 |
| Die Attach | Thickness | 0.030 |
| Bottom Die | Thickness | 0.130 |
| | Size | 12×12 |
| Underfill | Thickness | 0.090 |
| Mold | Thickness | 0.540 |
| Substrate | Thickness | 0.168 |
| | Size | 14×14 |
| Substrate Mask | Thickness | 0.030 |
| | Mask Opening Diameter | 0.3254 |
| Substrate Pad | Thickness | 0.027 |
| | Diameter | 0.1881 |
| SMD | Thickness | 0.030 |
| Solder Ball | Height | 0.300 |
| | Pitch | 0.800 |
| | Diameter | 0.400 |
| Printed Circuit Board | Thickness | 1.570 |
| | Size | 50×50 |
| PCB Mask | Thickness | 0.040 |
| | Mask Opening Diameter | 0.500 |
| Board Pad | Thickness | 0.027 |
| | Diameter | 0.300 |

Table 2.1 shows the dimensions of the typical flip chip package used in the analysis. The top die has a thickness of 0.100 mm and the size of the die is 9×9 mm square. Underneath the top die is the die attach with a layer thickness of 0.030 mm. The top die and die attach is placed above the bottom die which has a thickness of 0.130 mm with a die size of 12×12 mm square. Beneath the bottom die is a 0.090 mm thick layer of underfill which connects the bottom die to the package substrate. The mold encompasses the top and bottom dies as shown in Fig. 2.2 with a thickness of 0.540 mm from the substrate. The package substrate surfaces have a 0.030 mm thick substrate mask. Other details at the solder ball joint interfaces include a 0.027 mm thick substrate pad with a diameter of 0.1881 mm and a 0.027 mm thick board pad with a diameter of 0.300 mm. The solder ball itself has a standoff height of 0.300 mm, a pitch of 0.800 mm and a diameter of 0.400 mm. The printed circuit board is a 50×50 mm square board with a thickness of 1.570 mm. The printed circuit board surfaces also have PCB masks of 0.040 mm thick.

## 2.2 Solder Ball Fatigue Models

Viscoplastic finite-element simulations methodologies are utilized to predict the stress level and accumulated strain energy density per thermal cycle within the critical solder ball of a package. Two models with different levels of package details are used for the simulations. The first model is a simplified version of the flip chip package where a few layer details are omitted from the simulation model. The second model is a full model with more layer details incorporated into the simulation model. Omission of a few layer details at the interface of the model is carried out in order to determine if model simplification can produce results similar to a more complex model. For the simplified model only the most necessary basic components of the package are drawn

and many small details at the solder ball interfaces are neglected, with a possible view of obtaining results with much less effort. Due to the complex physics that encompass this type of non-linear transient finite element analysis, only half of a diagonal slice of the package was modeled in order to facilitate reasonable model run times. The utilization of a half diagonal slice assures that a worst-case situation is simulated where the perimeter solder ball is the farthest bump from the package centre neutral point shown in Fig. 2.1. The half diagonal slice representing the finite element model is shown by the diagonal bold print dashed line in Fig. 2.1.

The half diagonal slice model goes through the thickness of the overall package assembly, taking into account all major components and a full set of halved solder joints. Utilization of a slice model necessitates the consideration of boundary constraints that has to be imposed on the slice model, which has to appropriately represent the actual boundary conditions by which the full package assembly is subjected to. The symmetrical diagonal plane remains planar and constant in the y-direction throughout the analysis. The opposite side of the diagonal symmetric plane is neither a free surface nor a true symmetry plane. A reasonable compromise is to couple the y-displacements of the nodes on the slice plane. The effect of this constraint is that the slice plane is free to move in the y-direction, but that the surface is required to remain planar. Boundary constraints applied to a typical slice model are shown in Fig. 2.6. For all models presented in this work, the printed circuit board length is truncated at a distance after the package length. For a diagonal slice model, the ball pitch is the hypotenuse (1.1314mm) of the true ball pitch (0.80mm). The y-dimension or width of the slice model is one-half the solder ball pitch (0.5657mm).
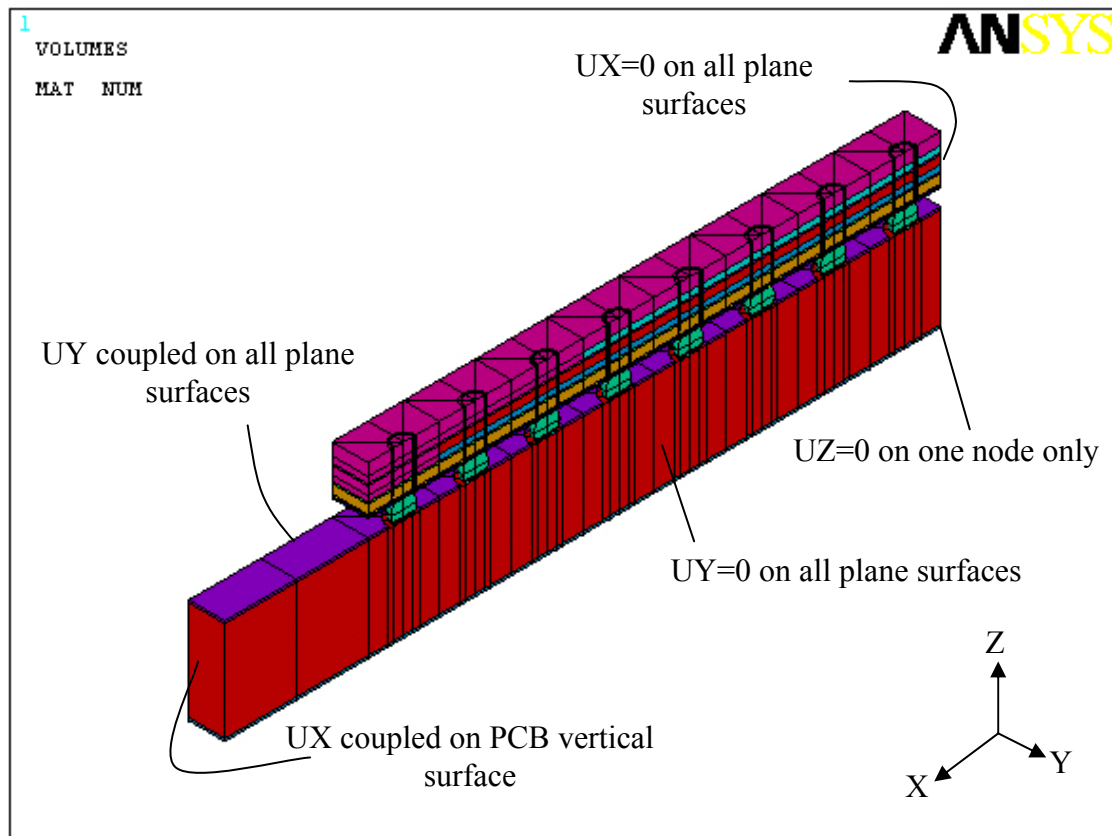
**Fig. 2.6.** Boundary constraints applied to a typical slice model (Zahn, 2000a).
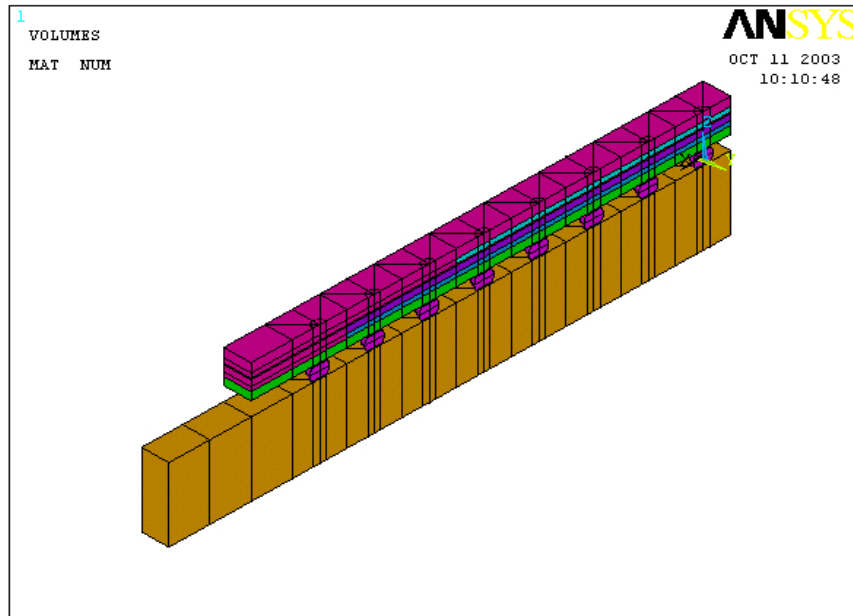
### 2.2.1 Simplified Flip Chip Model

A simplified flip chip model is used for the first part of the simulation. The layer configuration of the model is shown in Fig. 2.2. By comparing Fig. 2.2 with Figs. 2.3 through 2.5, a few details of the flip chip package assembly are omitted from this model. The solder mask layers on the substrate and on the printed circuit board are not included in this model. The substrate pads and the board pads are not included as well. The solder mask defined (SMD) layer on top of the solder balls is also omitted from the model. This configuration simplifies considerably the finite element model at the solder ball joints and hence reduces the modeling and computational time required.

Based on Table 2.1, a three dimensional model of the flip chip package is drawn using the commercial software ANSYS$^{\text{TM}}$ 7.0. The half diagonal slice finite element

model and the resulting mesh are shown in Figs. 2.7 and 2.8 respectively. The close-up details at one of the solder ball joint and its resulting mesh are shown in Figs. 2.9 and 2.10 respectively.



**Fig. 2.7.** Simplified diagonal slice model of the flip chip package.
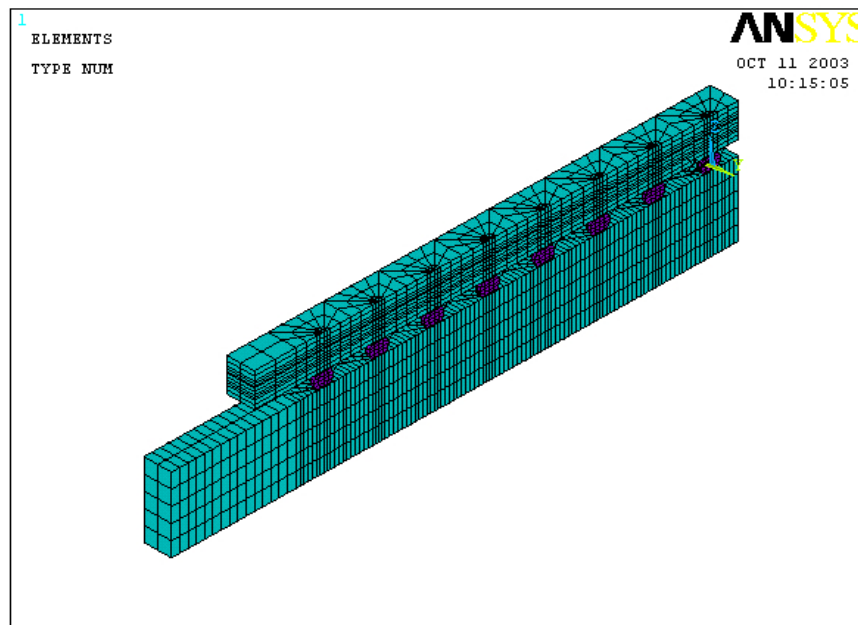


**Fig. 2.8.** Meshed simplified slice model of the flip chip package.
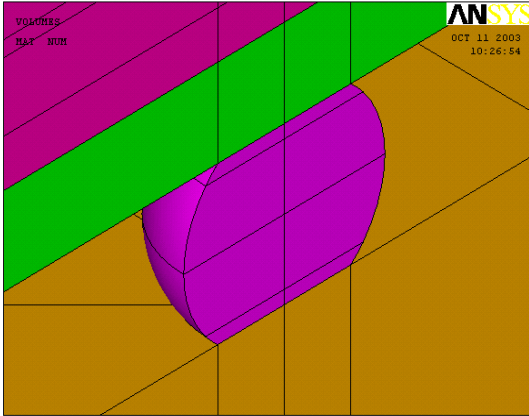
**Fig. 2.9.** Close-up details of a solder ball joint.
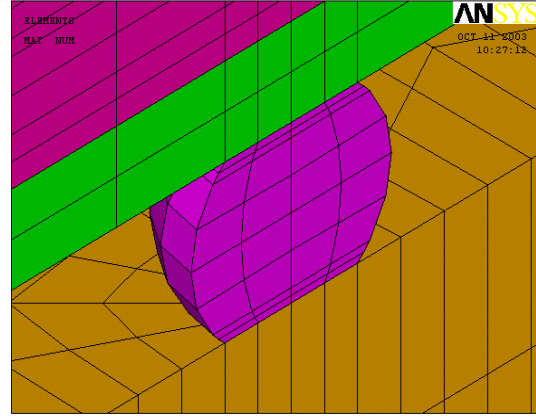
**Fig. 2.10.** The resulting mesh of a solder ball joint.

The entire model utilized a mapped or structured finite element mesh with 5506 elements and 7652 nodes. Typical solution run times are about 1.15 hours to 1.3 hours depending on the accelerated temperature cycling test condition applied.

### 2.2.2 Detailed Flip Chip Model

For the second part of the simulation, a more detailed flip chip model is used for simulation. As shown in Fig. 2.5, the SMD layer on top of each solder ball joints is included in the model. The substrate pads and the board pads along with the solder mask layers on the substrate and printed circuit board are included in the model. Based on Table 2.1 and Figs. 2.2 through 2.5, a three dimensional model of the flip chip package is drawn i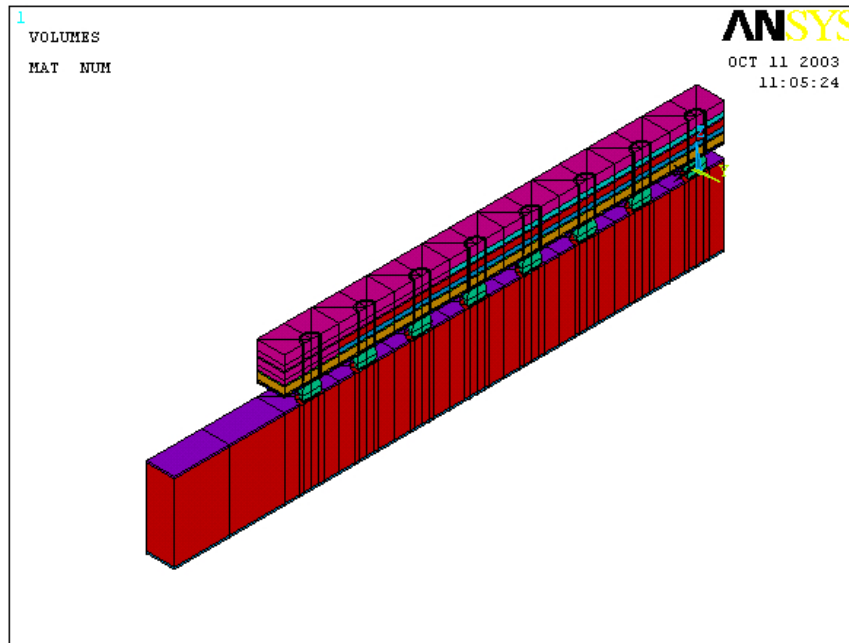n ANSYS$^{TM}$ 7.0. The half diagonal slice finite element model and the resulting mesh are shown in Figs. 2.11 and 2.12 respectively. The close-up details at one of the solder ball joints and its resulting mesh are shown in Figs. 2.13 and 2.14 respectively

**Fig. 2.11.** Detailed diagonal slice model of the flip chip package.



**Fig. 2.12.** Meshed detailed slice model of the flip chip package.

**Fig. 2.13.** Close-up details of a solder ball joint for the detailed model.

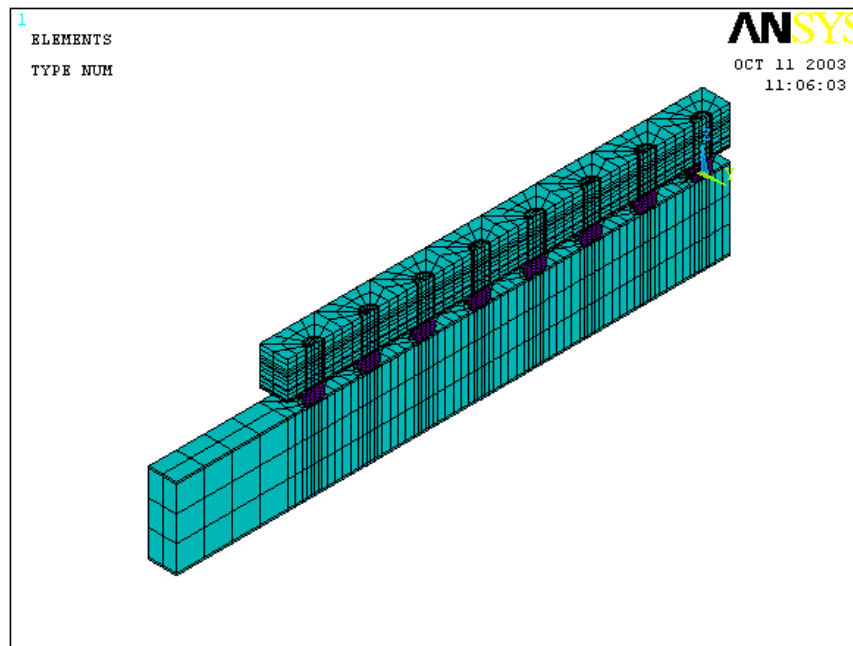**Fig. 2.14.** The resulting mesh of a solder ball joint for the detailed model.

The entire model utilized a mapped or structured finite element mesh with 6920 elements and 9308 nodes. Typical solution run times are about 1.25 hours to 1.42 hours depending on the accelerated temperature cycling test condition applied.
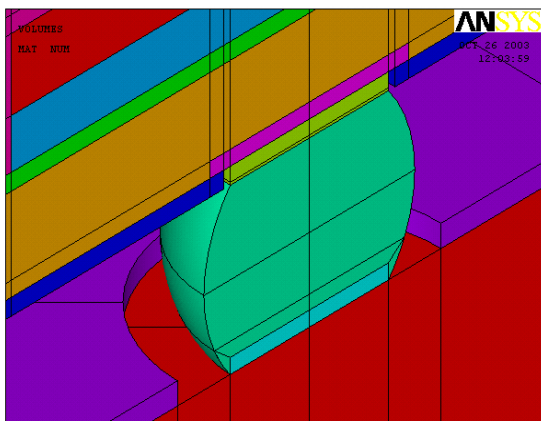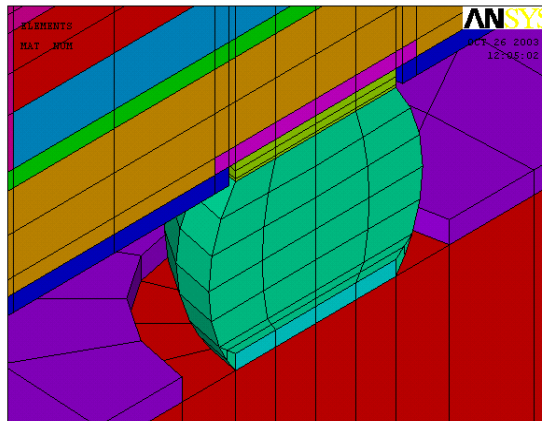
## 2.3 Material Properties and Modified Anand Constants

Tables 2.2 through 2.8 show the material properties incorporated in the finite element models. As seen from the tables, most of the properties used in the analysis are dependent only on temperature.

**Table 2.2.** Die material properties (Intel).

| Temp. (K) | Young's Modulus (MPa) | Temp. (K) | CTE (1/K) | Poisson's Ratio |
|-----------|-----------------------|-----------|-----------|-----------------|
| 213 | 131000 | 200 | 2.36E-6 | 0.279 |
| 233 | 131000 | 250 | 2.63E-6 | |
| 273 | 130000 | 293 | 2.81E-6 | |
| 293 | 130000 | 325 | 2.89E-6 | |
| 323 | 130000 | 350 | 2.98E-6 | |
| 373 | 129000 | 425 | 3.3E-6 | |
| 500 | 129000 | 450 | 3.5E-6 | |
| | | 500 | 3.61E-6 | |

**Table 2.3.** Die attach/underfill material properties (Intel).

| Young's Modulus (MPa) | CTE (1/K) | Poisson's Ratio |
|---|---|---|
| $-268349 + 4631.4T - 32.27T^2 + 0.117T^3 - 0.0002T^4 + 2\times10^{-7}T^5 - 1\times10^{-10}T^6$ | $-0.028 + 0.0005T - 4\times10^{-6}T^2 + 1\times10^{-8}T^3 - 3\times10^{-11}T^4 + 3\times10^{-14}T^5 - 1\times10^{-17}T^6$ | 0.3 |

**Table 2.4.** Mold material properties (Intel).

| Temp. (K) | Young's Modulus (MPa) | Temp. (K) | CTE (1/K) | Poisson's Ratio |
|---|---|---|---|---|
| 233 | 21300 | 223 | 1.545E-5 | 0.3 |
| 273 | 19900 | 410 | 5.020E-5 | |
| 298 | 19000 | 435.5 | 3.901E-5 | |
| 323 | 18100 | 573 | 4.192E-5 | |
| 373 | 16100 | | | |
| 423 | 2200 | | | |
| 498 | 600 | | | |

**Table 2.5.** Substrate material properties (Intel).

| Young's Modulus (MPa) | Shear Modulus (MPa) | CTE (1/K) | Poisson's Ratio |
|---|---|---|---|
| $29664 - 39.455T$ (X,Y)<br>7800 (Z) | 1520 (X,Y)<br>152 (Z) | $1.6\times10^{-5}$ (X,Y)<br>$6\times10^{-5}$ (Z) | 0.39 (X,Y,Z) |

**Table 2.6.** Solder ball material properties (Intel).

| Young's Modulus (MPa) | CTE (1/K) | Poisson's Ratio |
|---|---|---|
| $75827 - 151.64T$ | $2\times10^{-5} + 2\times10^{-8}T$ | 0.35 |

**Table 2.7.** Printed circuit board material properties (Intel).

| Young's Modulus (MPa) | Shear Modulus (MPa) | CTE (1/K) | Poisson's Ratio |
|---|---|---|---|
| $29664 - 39.455T$ (X,Y)<br>7800 (Z) | 1520 (X,Y)<br>152 (Z) | $1.6\times10^{-5}$ (X,Y)<br>$6\times10^{-5}$ (Z) | 0.39 (X,Y,Z) |

**Table 2.8.** Substrate mask/PCB mask material properties (Intel).

| Young's Modulus (MPa) | CTE (1/K) | Poisson's Ratio |
|:---:|:---:|:---:|
| 4137 | $30\times10^{-6}$ | 0.40 |

T is material properties temperature in Kelvin

## 2.3.1 Anand's constitutive model and Darveaux's constitutive model

Anand (1982) presented a constitutive model to describe the deformation of metals at elevated temperature. Anand's model is described by equations (1) to (4).

$$\frac{d\varepsilon_p}{dt} = A\exp\left(-\frac{Q}{kT}\right)\left[\sinh\left(\xi\frac{\sigma}{s}\right)\right]^{1/m} \tag{1}$$

$$\frac{ds}{dt} = \left[h_o\left(|B|\right)^{a'}\frac{B}{|B|}\right]\frac{d\varepsilon_p}{dt} \tag{2}$$

$$B = 1 - \frac{s}{s^*} \tag{3}$$

$$s^* = s^{\wedge}\left[\frac{d\varepsilon_p/dt}{A}\exp\left(\frac{Q}{kT}\right)\right]^n \tag{4}$$

where $\dfrac{d\varepsilon_p}{dt}$ is the effective inelastic deformation rate

$s$ is the initial value of deformation resistance

$Q/k$ is the activation energy/Boltzmann's constant

$A$ is the pre-exponential factor

$\xi$ is the multiplier of stress

$m$ is the strain rate sensitivity of stress

$h_o$ is the hardening constant

$s^{\wedge}$ is the coefficient for deformation resistance saturation value

*n*      is the strain rate sensitivity of saturation value

*a'*     is the strain rate sensitivity of hardening

Anand's constitutive relations are proposed for rate-dependent viscoplasticity model. Plasticity is defined by the propensity of a material to undergo permanent deformation under load. Viscoplasticity is defined when creep is taken into consideration with plasticity. Anand's model however does not consider rate-independent plasticity.

Darveaux (2000) has through his work presented his constitutive relations that describe the deformation behaviour of solder joints through equations (5) to (9) as shown below. Steady state creep of solder is expressed by the relationship of

$$\frac{d\varepsilon_s}{dt} = C_{ss}\left[\sinh(\alpha\sigma)\right]^n \exp\left(-\frac{Q_a}{kT}\right) \tag{5}$$

where $\dfrac{d\varepsilon_s}{dt}$ is the steady state strain rate, $k$ is the Boltzmann's constant, $T$ is the absolute temperature, $\sigma$ is the applied stress, $Q_a$ is the apparent activation energy, $n$ is the stress exponent, $\alpha$ prescribes the stress level at which the power law dependence breaks down, and $C_{ss}$ is a constant.

Transient creep at constant stress and temperature can be described by

$$\varepsilon_c = \frac{d\varepsilon_s}{dt}t + \varepsilon_T\left(1 - \exp\left(-B\frac{d\varepsilon_s}{dt}t\right)\right) \tag{6}$$

where $\varepsilon_c$ is the creep strain, $\dfrac{d\varepsilon_s}{dt}$ is the steady state creep rate, $\varepsilon_T$ is the transient creep strain, and $B$ is the transient creep coefficient.

The instantaneous creep rate is given by

$$\frac{d\varepsilon_c}{dt} = \frac{d\varepsilon_s}{dt}\left(1 + \varepsilon_T B \exp\left(-B\frac{d\varepsilon_s}{dt}t\right)\right) \tag{7}$$

where $\dfrac{d\varepsilon_s}{dt}$ is the steady state creep rate.

There is also a time-independent plastic strain component to the deformation at high stresses when $\tau/G > 10^{-3}$.

$$\varepsilon_p = C_p\left(\frac{\sigma}{G}\right)^{m_p} \tag{8}$$

where $\varepsilon_p$ is the time-independent plastic strain, $G$ is the shear modulus, and $C_p$ and $m_p$ are constants. This component is not considered in Anand's model. The total inelastic strain is given by the sum of creep strain and plastic strain

$$\varepsilon_{in} = \varepsilon_c + \varepsilon_p \tag{9}$$

where $\varepsilon_{in}$ is the total inelastic strain.

As mentioned earlier, equation (8) is the time-independent plastic strain which has not been taken into consideration by Anand's model as Anand's model is only meant for a rate-dependent plasticity approach. Darveaux's model however incorporates